Inorganic Chemistry

ARTICLE

pubs.acs.org/IC

Novel Fluorous Amphiphilic Heteroleptic Ru-Based Complexes for a Dye-Sensitized Solar Cell: The First Fluorous Bis-ponytailed Amphiphilic Ru Complexes

Norman Lu,*[,†] Jia-Sheng Shing,[†] Wen-Han Tu,[†] Ying-Chan Hsu,[‡] and Jiann T. Lin*[,‡]

[†]Institute of Organic and Polymeric Materials, National Taipei University of Technology, Taipei 106, Taiwan

[‡]Institute of Chemistry, Academia Sinica, Taipei 115, Taiwan

Supporting Information

ABSTRACT: A new series of amphiphilic heteroleptic ruthenium(II) sensitizers with a fluorous bis-ponytailed bipyridine ancillary ligand, [Ru(H_2dcbpy)(4,4′-bis($R_fCH_2OCH_2$)-2,2′-bpy)$(NCS)_2$] [where R_f = HCF_2CF_2 (**CT4**), C_3F_7 (**CT7**), and $HCF_2CF_2CF_2CF_2$ (**CT8**)], have been synthesized and fully characterized by UV/vis, visible emission, NMR, fast atom bombardment mass spectrometry, and cyclic voltammetric studies. Dye-sensitized solar cells (DSCs) based on these dyes exhibit efficiencies comparable with that of the standard cell based on **N719**. The conversion efficiency of a **CT7**- or **CT8**-based DSC is ∼9% higher than that of **Z907** with a nonfluorous bis-ponytailed bipyridine ancillary ligand. The fluorous chains were found to increase the dye density on TiO_2 and to help to suppress the dye desorption.

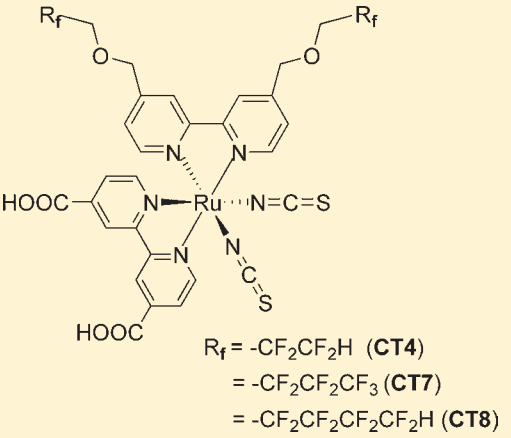

INTRODUCTION

Sensitizers of low cost and good efficiency have a great potential to be used in nanocrystalline dye-sensitized solar cells (DSCs).[1,2] DSCs based on metal-free organic sensitizers possessing very high extinction coefficients have been reported to exhibit power conversion efficiencies surpassing 9%.[3,4] In comparison, several polypyridylruthenium(II)-based DSCs have even higher efficiencies of >11% under standard AM 1.5 sunlight.[5−10] Up to now, very few amphiphilic heteroleptic ruthenium complexes[11] (e.g., **Z907**; Figure 1) were reported to have enough stability under prolonged light soaking and thermal stress at 80 °C when used in solid-state DSCs. However, the lower molar extinction coefficient of the metal-to-ligand charge transfer (MLCT) band of **Z907** compared to that of homoleptic dye *cis*-dithiocyanato(bis-2,2′-bipyridyl-4,4′-dicarboxylate)ruthenium(II) (**N719**; Figure 1)[12] leads to a lower cell efficiency of the former than of the latter. That is, there is trade-off between the efficiency and stability of the **Z907**-based DSC.[11] Although an extended π-conjugated system may benefit the DSC efficiency because of its higher molar extinction coefficient,[12] an increment in the size accompanying the extended π conjugation may also result in lower dye adsorption. It should be attractive to develop effective simple amphiliphilic transition-metal-based sensitizers tolerant toward thermal stress and light soaking for future solar cell applications. Herein we report the successful synthesis and full characterization of three novel fluorous amphiphilic ruthenium complexes, as shown in Figure 1. To our knowledge, this is the first report on ruthenium sensitizers containing fluorous bis-ponytailed 2,2′-bipyridine (bpy) ancillary ligands.[13] Because moisture was reported to be detrimental[11] to the affinity of dye to TiO_2, an enhanced stability is expected by attaching the extremely hydrophobic fluorous spectator to the bpy ring.

RESULTS AND DISCUSSION

The 4,4′-bis($R_fCH_2OCH_2$)-2,2′-bpy ligand,[14] where R_f = HCF_2CF_2 (**CT4**), C_3F_7 (**CT7**), and $HCF_2CF_2CF_2CF_2$ (**CT8**), was synthesized from the reaction of 4,4′-bis(CH_2Br)-2,2′-bpy and fluorinated alkoxide, R_fCH_2ONa. These ligands were then used in the two-stage synthetic procedure[15] developed for heteroleptic polypyridylruthenium complexes. Complexes **CT4**, **CT7**, and **CT8** (Figure 1) were isolated in moderate yields (∼32%). Further synthetic details and analytical data are provided in the Experimental Section.

The pertinent photophysical data are displayed in Table 1. The UV/vis spectra of **CT4**, **CT7**, **CT8**, and **N719** in *N*,*N*-dimethylformamide (DMF) are shown in Figure 2. The low-energy MLCT bands of the dyes **CT4**, **CT7**, and **CT8** at ca.

Received: October 31, 2010
Published: April 14, 2011

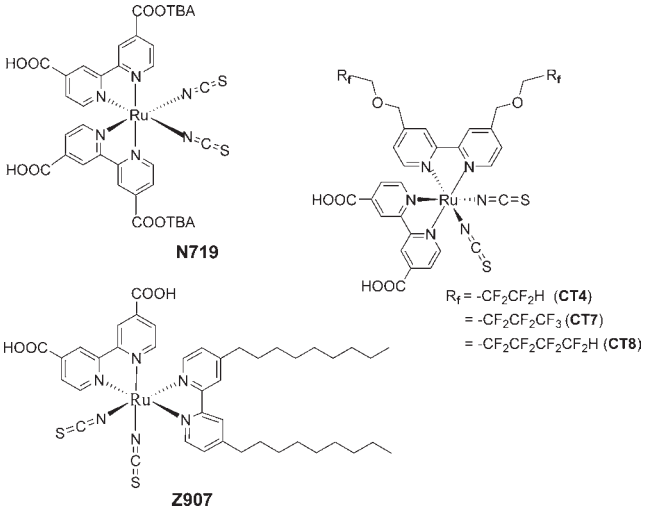

Figure 1. Molecular structures of **N719**, **Z907**, and the CT dye series (**CT4**, **CT7**, and **CT8**).

Table 1. Absorption and Photophysical Properties of the Ruthenium Sensitizers

	absorption maximum (nm) [ε ($\times 10^4$ M^{-1} cm^{-1})]			
dye[a]	$\pi-\pi^*$	$\pi-\pi^*$	$d\pi-\pi^*$	emission (nm)
CT4	299 (5.86)	370 (1.47)	519 (1.25)	737
CT7	298 (6.33)	370 (1.46)	520 (1.24)	745
CT8	299 (5.88)	370 (1.46)	520 (1.25)	736
N719[b]	312 (4.26)	385 (1.23)	532 (1.40)	830
Z907[c,d]	297 (5.12)[c]	372 (1.33)[c]	525 (1.26)[c]	769[d]

[a] Absorption and emission data were recorded in DMF solutions. [b] **N719** data are from both ref 19 and this work. [c] The UV/vis spectrum (e.g., MLCT data) of **Z907** in DMF has been measured under the same conditions in this work. [d] **Z907** data from refs 11 and12.

525 nm have molar extinction coefficients of 12.5×10^3, 12.4×10^3, and 12.5×10^3 M^{-1} cm^{-1}, respectively. These values are lower than the corresponding value of the standard **N719** dye (14.0×10^3 M^{-1} cm^{-1}) and are about the same as that of **Z907** (12.6×10^3 M^{-1} cm^{-1}).[16,17] The emission maxima (λ_{ex} = 520 nm) appeared at 737, 745, 736, and 830 nm for **CT4**, **CT7**, **CT8**, and **N719**, respectively, as shown in Figures S4.1−S4.3 (see the Supporting Information, SI). From the combined normalized UV/vis and emission spectra (see the SI), the E_{0-0} excitation transition energies (Table 2) were then estimated to be 1.91, 1.90, 1.88, 1.86, and 1.64 eV[16] for **CT4**, **CT7**, **CT8**, **N719**, and **Z907**, respectively.

Cyclic voltammetry (CV) was used to measure the redox potential of these fluorous sensitizers, and the pertinent data in DMF are shown in Tables 1 and 2. The first reversible oxidation potential (E_{ox}) ranging from 0.35 to 0.39 V with reference to ferrocene can be assigned to the Ru^{II}/Ru^{III} couple. The E_{ox} value of **CT4** (0.35 V), **CT7** (0.38 V), or **CT8** (0.39 V) is attributed to its electron-withdrawing fluorous chain, which renders the Ru center slightly electron-deficient. In contrast, the corresponding CV peak of **Z907** containing an electron-releasing nonyl group, C_9H_{19}, occurs at 0.28 V.[18] The highest occupied molecular orbital (HOMO) energy levels of **CT4**, **CT7**, **CT8**, **N719**,

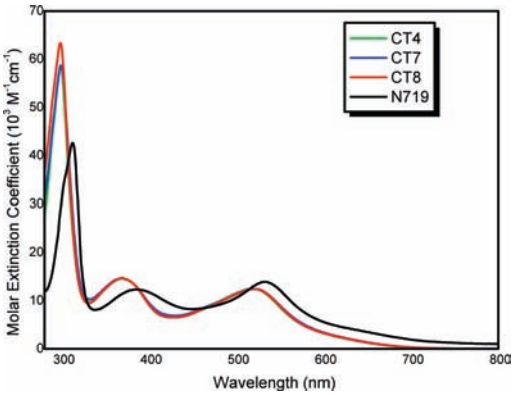

Figure 2. UV/vis spectra of **CT4**, **CT7**, **CT8**, and **N719** in DMF.

and **Z907** are calculated to be −5.15, −5.18, −5.19, −5.16, and −5.08 eV, respectively. These values are lower than that[18] (−4.9 eV) of the I^-/I_3^- pair and provide ample driving force for efficient dye regeneration and thus net charge separation. The E_{0-0}* energy levels of **CT4**, **CT7**, and **CT8** were calculated to be −3.24, −3.28, and −3.31 eV, respectively. These values are similar to that of **Z907** (estimated as −3.44 eV) and higher than that of the TiO_2 conduction band edge, which ensures enough driving force for electron injection. The energy level diagrams of these dyes are shown in Scheme 1.

DSCs were fabricated using these dyes as the sensitizers, with an effective area of 0.25 cm^2, nanocrystalline anatase TiO_2 particles, and an electrolyte composed of 0.05 M I_2/0.5 M LiI/0.5 M *tert*-butylpyridine in an acetonitrile solution. The performance statistics of the DSCs fabricated using these dyes as sensitizers under AM 1.5 illumination are listed in Table 3. Figure 3 shows the photocurrent−voltage ($I-V$) curves and the incident photocurrent conversion efficiencies (IPCEs) of the cells. The IPCE values that peak at ~540 nm are 70, 70, and 70% for **CT7**, **CT8**, and **N719**, respectively. The maximum IPCE previously reported for **N719** was 85%.[19,20] It is interesting to note that dye **CT7** shows a better IPCE than **N719** in the excitation range of 420−540 nm, and **CT8** is also superior to **N719** from 440 to 600 nm. Nevertheless, the open circuit voltages (V_{oc}) of **CT7** and **CT8** are slightly smaller than that of **N719**. The efficiencies (see Table 3) of **CT7** and **CT8** are close to that of **N719** and are ca. 9% higher than that of **Z907**, whose IPCE curve is slightly red-shifted. These results are especially interesting given the similar molar extinction coefficients of **CT7** (or **CT8**) and **Z907**. Obviously, the fluorous ponytail on the amphiphilic sensitizers is beneficial to the cell efficiency.

With nearly similar absorption profile and intensity among CT4, CT7 and CT8, we speculate the different adsorption abilities of the dyes are the main cause of different cell efficiencies. In order to clarify this assumption, adsorption tests were carried out and the results are shown in Table 4. The fluorous chains from the ancillary bpy have extra adsorption ability[20] toward TiO_2 surface compared with the normal long alkyl chains on Z907. In viewing that the polyfluorinated CF_2 groups are capable of forming C−F···H−C hydrogen bonding, it is conceivable that the CF_2 (or CF_3) groups and/or the acidic H from $-HCF_2$ group can form weak hydrogen bonds[21] with −OH groups at the TiO_2 surface. Such multipoints bonding mode may help suppress dye leaching and thus increase the adsorbed dye density. As

dx.doi.org/10.1021/ic102192m |*Inorg. Chem.* 2011, 50, 4289–4294

Table 2. Electrochemical Data and Molecular Orbital Properties of CT4, CT7, CT8, N719, and Z907

dye	E_{ox} (V)	$E_{ox} - E_{Fc/Fc+}$ (V)	HOMO (eV)	E_{0-0} (eV)[a]	E_{0-0}* (eV)
CT4	0.92 (±0.067)	0.35	−5.15	1.91	−3.24
CT7	0.95 (±0.052)	0.38	−5.18	1.90	−3.28
CT8	0.96 (±0.055)	0.39	−5.19	1.88	−3.31
N719	0.89 (±0.065)	0.36	−5.16	1.86	−3.30
Z907[b]	0.74[b] (±0.080)	0.28 [b]	−5.08	1.64 [c]	−3.44 [c]

[a] E_{0-0}, calculated from equation $E_{0-0} = 1240/\lambda$, is the excitation transition energy, which is used as the estimated energy gap, E_g. HOMO = $-(4.8 + E_{ox} - E_{Fc/Fc+})$; E_{0-0}* = E_{0-0} + HOMO. [b] **Z907** data from ref 16a. [c] E_{0-0}* of **Z907** from ref 16c.

Scheme 1. Energy Level Diagrams of CT8, CT7, CT4, N719, Z907, TiO_2, and I^-/I_3^-

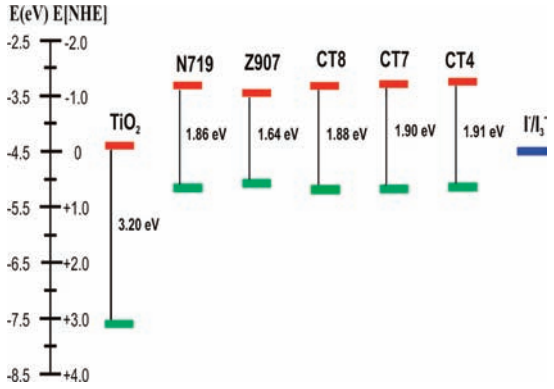

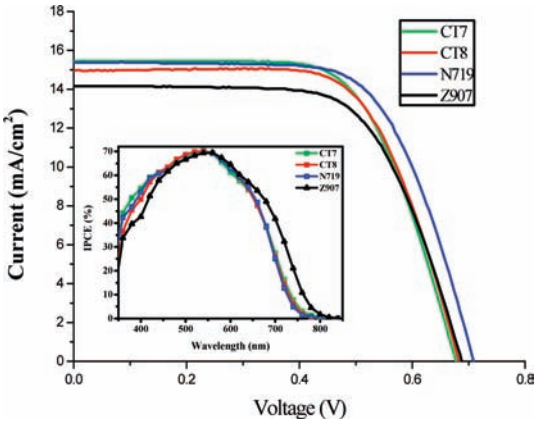

Figure 3. *I*−*V* curve and IPCE diagram of dyes **CT7**, **CT8**, **N719**, and **Z907** (for clarity, the **CT4** data are omitted).

Table 3. Detailed Photovoltaic Parameters of Cells Made with CT4, CT7, CT8, N719, and Z907

cell	V_{oc} (V)	J_{SC} (mA cm^{-2})	FF	η (%)
CT4	0.67	−13.33	0.70	6.25
CT7	0.68	−15.44	0.66	6.93
CT8	0.68	−14.98	0.67	6.82
N719[a]	0.71	−15.37	0.67	7.31[a]
Z907	0.68	−14.16	0.66	6.36

[a] The **N719** efficiency of 7.31% was obtained under our conditions as opposed to 11.18% reported in ref 10. Light intensity: 100 mW cm^{-2} (1.5 AM).

shown in Table 4, the adsorbed packing density of each dye is calculated[22] from the difference in dye concentration before and after TiO_2 film immersion. Both CT7 and CT8 have much higher dye packing density than that of Z907. The slightly lower dye concentration of CT4 may be due to its lower number of F atoms (4 Fs on each side) available. With longer fluorous chains, there are stronger interaction between the TiO_2 and the fluorous dye, and consequently higher dye adsorption. The order of dye density is in parallel with the cell efficiency (Table 3).

In addition, the IR spectral studies of the tetrabutylammonium (TBA) salts of three free dyes and their TiO_2 adsorbed dyes were also carried out to prove interaction of the polyfluorinated chain with the TiO_2 surface. When the free and adsorbed CT4 salts (shown in Figure 4) are compared as an example, the asymmetric (ν_{as}) and symmetric (ν_s) stretchings of CF_2 groups are shifted from 1203 and 1107 cm^{-1} in the free **CT4** salt to 1233 and 1116 cm^{-1} in the adsorbed **CT4** salt, respectively; the shift of the stronger CF_2 stretching (ν_s) of the **CT4** salt before and after binding to the TiO_2 surface is as much as 9 cm^{-1} (1116 vs 1107 cm^{-1}). In contrast, the symmetric stretching of the COO^- group from the **CT4** salt was shifted from 1356 to 1385 cm^{-1}, as reported in the literature,[23,24] when the **CT4** salt is bound to the TiO_2 surface. The NCS asymmetric stretching was hardly shifted in both the top and bottom spectra. Thus, the change of the vibrational position of the CF_2 group was an indication of the structural change of the dye molecule. This structural change of the dye molecule should result from adsorption of the polyfluorinated chain on the TiO_2 surface. As for the salts of **CT7** and **CT8**, both also showed similar shifting results (see Figures S5 and S6 in the SI) of CF_2 (or CF_3) stretchings measured under attenuated total reflectance (ATR) mode when these two dye salts were bound to the TiO_2 surface. Therefore, these data further substantiate our argument that there exists a weak interaction between the polyfluorinated chain and the −OH group on the TiO_2 surface. Thus, all of these three polyfluorinated dyes were more strongly bound to the TiO_2 surface than **Z907**.

The dark current (Figure 5) decreases in the order of increasing length of the fluorous ponytail, i.e., **CT4** > **CT7** > **CT8**. Whether the longer fluorous ponytail is more effective in suppressing the dark current needs further study.[25] Moreover, dye leaching by moisture is also eased. In addition, the dye desorption studies showed that both adsorbed **Z907** and adsorbed **N719** could be easily flushed away from the TiO_2 surface by rinsing with a 5 M NaOH aqueous solution, while negligible

dx.doi.org/10.1021/ic102192m |*Inorg. Chem.* 2011, 50, 4289–4294

Table 4. Adsorption Test

	CT4	CT7	CT8	N719	Z907
dye soln concn before TiO_2 immersion ($\times 10^{-4}$ M)	3.00	3.00	3.00	3.00	3.00
dye soln concn after TiO_2 immersion ($\times 10^{-4}$ M)	2.75	2.66	2.62	2.68	2.85
moles of adsorbed dye on TiO_2 ($\times 10^{-7}$ M)	2.50	3.40	3.80	3.20	1.50
wt (mg) of (TiO_2 + adsorbed dye)	3.40	3.26	3.70	3.53	3.26
dye adsorbed ($\times 10^{-7}$ mol cm^{-2})[a]	1.76	2.50	2.46	2.18	1.10

[a] Equation for the amount of dye adsorbed = [moles of adsorbed dye on TiO_2/wt of (TiO_2 + adsorbed dye)] × 2.40.

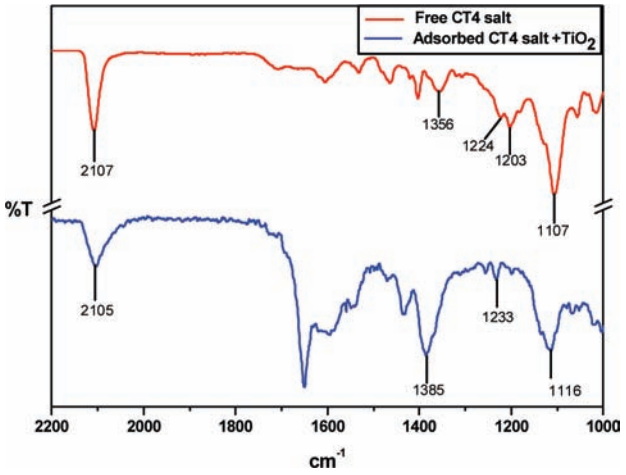

Figure 4. ATR-FT-IR spectra of the free (top) and adsorbed (bottom) **CT4** salts [the **CT4** salt used for the IR study here is its TBA salt; its structure is tetrabutylammonium ruthenium (4,4′-bis(2,2,3,3-tetrafluoropropoxymethyl)-2,2′-bipyridine)(4-carboxylic acid-4′-carboxylate-2,2′-bipyridine)$(NCS)_2$].

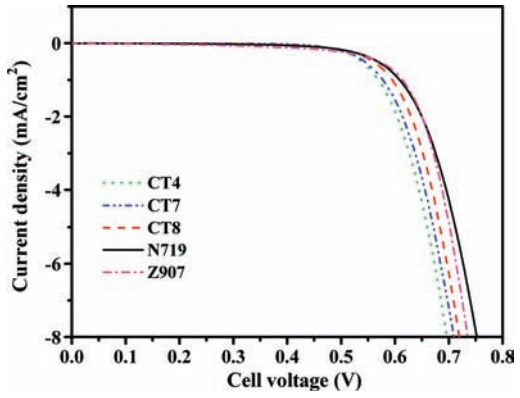

Figure 5. *I*−*V* curves of the DSCs measured in the dark.

dye desorption was observed for CT dye series after immersion in a concentrated NaOH solution.

CONCLUSIONS

In conclusion, new types of fluorous amphiphilic heteroleptic bipyridylruthenium complexes have been synthesized and were found to be efficient, stable sensitizers for nanocrystalline DSCs using a liquid electrolyte. The amphiphilic heteroleptic ruthenium(II) sensitizers, self-assembled on TiO_2 surfaces from a tetrahydrofuran (THF) solution, reveal efficient sensitization in the visible range. Both **CT7** and **CT8** yielded even higher IPCEs than standard **N719** at 540 nm. Instead of using an extending π-conjugated system, our simple fluorous amphiphilic dyes, **CT7** and **CT8**, exhibit efficiencies comparable with that of the homoleptic standard **N719** dye and better than that of **Z907**. The hydrophobic polyfluorinated chains in these new dyes not only lead to higher dye density on TiO_2 but also suppress dye leaching. The better cell efficiency and dye durability of these polyfluorinated dyes than their nonfluororinated congener, **Z907**, shed light on the direction for the design of new dyes in the future. Utilization of these new sensitizers for quasi-solid-state and solid-state applications will also be explored in the future.

EXPERIMENTAL SECTION

Materials. All reagents were obtained from commercial sources and used as received unless specified otherwise. Solvents were dried over sodium or CaH_2 before use. The fluorous ligands were synthesized as reported in the earlier publication. The structures of dyes **CT4**, **CT7**, and **CT8** and their intermediates were identified with multinuclei NMR spectra. Samples analyzed by fast atom bombardment (FAB) mass spectroscopy (MS) were done by the staff of the National Central University (Taiwan) mass spectrometry laboratory. IR spectra were obtained on a Perkin-Elmer RX I FT-IR spectrometer; and ATR data reported here were taken with an ATR accessory (Pike Technology) with a ZnSe crystal plate using typically 32 scans at a resolution of 4 cm^{-1}. The samples were all measured under the same mechanical force pushing the samples in contact with the window. UV/vis spectra were recorded on a Shimadzu UV-360 spectrophotometer in a quartz cell with a 1 cm path length. The emission spectra were recorded in the range of 550−800 nm on a Fluoromax-4 spectrometer.

Synthesis of Ru[(dcbpy)(4,4′-bis($R_fCH_2OCH_2$)-2,2′-bpy)-$(NCS)_2$] (CT Series; See the SI for Drawings and Spectra). The **CT8** dye was synthesized with a typical one-pot synthesis procedure reported previously.[15] $[RuCl_2(p\text{-cymene})]_2$ (0.62 mmol, 0.38 g) and 4,4′-bis($HC_4F_8CH_2OCH_2$)-2,2′-bpy[2] (1.24 mmol, 0.8 g) were dissolved in 60 mL of ethanol, and then the solution was stirred and refluxed for 8 h at 80 °C under a N_2 atmosphere. After ethanol was pumped away, 4,4′-dicarboxylic acid-2,2′-bipyridine (dcbpy; 1.24 mmol, 0.30 g) and 40 mL of dry DMF were added. The reaction mixture was refluxed at 140 °C for another 4 h in the dark to avoid light-induced cis-to-trans isomerization. Excess NH_4NCS was added to the reaction mixture and heated at 130 °C for 5 h. After the reaction, the solvent was removed with a rotary vacuum pump and a large amount of water was added to dissolve the excess NH_4NCS. The water-insoluble product was collected on a sintered glass crucible by water suction, washed with distilled water, followed by diethyl ether, and dried in oven at 60 °C. The crude product (89% yield) was treated with TBAOH, and then the resulting TBA salt was dissolved in methanol and then passed through a chromatography column (Sephadex LH20) using methanol as the

dx.doi.org/10.1021/ic102192m |*Inorg. Chem.* 2011, 50, 4289–4294

eluent. The main band was collected and concentrated. A few drops of 0.01 M HNO_3(aq) was added to precipitate the product. After recrystallization, pure **CT8** was obtained in 30% (0.414 g) yield (**CT7**, purified yield 31.6%; **CT4**, purified yield 32%).

Analytical Data of CT7. NMR: (500 MHz, CD_3OD) δ_H 9.61 (1H, d, $^3J_{HH}$ = 6.0 Hz, H^6), 9.37 (1H, d, $^3J_{HH}$ = 5.5 Hz, $H^{6\prime}$), 9.01 (1H, s, H^3), 8.86 (1H, s, $H^{3\prime}$), 8.49 (1H, s, $H^{3\prime\prime\prime}$), 8.34 (1H, s, $H^{3\prime\prime}$), 8.24 (1H, d, $^3J_{HH}$ = 5.5 Hz, $H^{5\prime}$), 7.85 (1H, d, $^3J_{HH}$ = 6.0 Hz, $H^{6\prime\prime\prime}$), 7.80 (1H, d, $^3J_{HH}$ = 6.0 Hz, $H^{5\prime\prime}$), 7.62 (1H, d, $^3J_{HH}$ = 6.0 Hz, H^5), 7.53 (1H, d, $^3J_{HH}$ = 6.0 Hz, $H^{6\prime\prime}$), 7.14 (1H, d, $^3J_{HH}$ = 6.0 Hz, $H^{5\prime\prime\prime}$), 5.08 (2H, s, $H^{8\prime\prime\prime}$), 4.80 (2H, s, $H^{8\prime\prime}$), 4.39 (2H, t, $^3J_{HF}$ = 14.0 Hz, $H^{9\prime\prime\prime}$), 4.19 (2H, t, $^3J_{HF}$ = 14.0 Hz, $H^{9\prime\prime}$); δ_F (470.5 MHz, CD_3OD) −122.0 (2F, br, $-CH_2\underline{C}F_2CF_2-$), −122.2 (2F, br, $-CH_2\underline{C}F_2CF_2-$), −129.1 (2F, m, $-CH_2CF_2\underline{C}F_2-$), −129.2 (2F, m, $-CH_2CF_2\underline{C}F_2-$), −82.9 (3F, t, $^3J_{FF}$ = 8.9 Hz, $-\underline{C}F_3$), −83.0 (3F, t, $^3J_{FF}$ = 8.5 Hz, $-\underline{C}F_3$); δ_C (113 MHz, CD_3OD) 167 (C^7), 167 ($C^{7\prime}$), 161 (C^2), 160 ($C^{2\prime}$), 160 ($C^{2\prime\prime}$), 158 ($C^{2\prime\prime\prime}$), 155 (C^6), 154 ($C^{6\prime}$), 154 ($C^{6\prime\prime}$), 153 ($C^{6\prime\prime\prime}$), 150 (C^4), 149 ($C^{4\prime}$), 140 ($C^{4\prime\prime}$), 140 ($C^{4\prime\prime\prime}$), 127 (C^3), 126 ($C^{3\prime}$), 126 ($C^{3\prime\prime}$), 125 ($C^{3\prime\prime\prime}$), 124 (C^5), 124 ($C^{5\prime}$), 122 ($C^{5\prime\prime}$), 122 ($C^{5\prime\prime\prime}$), 135 ($C^{13\prime}$ of NCS), 135 (C13 of NCS), 106−118 ($C^{10\prime\prime\prime}$−$C^{12\prime\prime\prime}$ and $C^{10\prime\prime}$−$C^{12\prime\prime}$), 73 ($C^{8\prime\prime\prime}$), 73 ($C^{8\prime\prime}$), 69 ($C^{9\prime\prime\prime}$), 68 ($C^{9\prime\prime}$). FT-IR (cm^{-1}): 2105 [ν(N═C), s], 1716 [ν(bpy-C═O), s], 1613 [ν_{as}(bpy-COO^-), s], 1617, 1542, 1406 [ν(bpy), m], 1383 [ν(bpy-CH_2O), m], 1169 [$\nu(CF_2)$, s], 1229 [ν(bpy-CO), s], 1129 [$\nu(CF_2)$, s]. HR-MS (FAB), M^+. Calcd for $C_{34}H_{22}F_{14}N_6O_6RuS_2$: m/z 1041.9870. Found: m/z 1041.9872.

Analytical Data of CT8. NMR: δ_H (500 MHz, CD_3OD) 9.61 (1H, d, $^3J_{HH}$ = 5.5 Hz, H^6), 9.36 (1H, d, $^3J_{HH}$ = 6.0 Hz, $H^{6\prime}$), 9.01 (1H, s, H^3), 8.86 (1H, s, $H^{3\prime}$), 8.49 (1H, s, $H^{3\prime\prime\prime}$), 8.34 (1H, s, $H^{3\prime\prime}$), 8.21 (1H, d, $^3J_{HH}$ = 6.0 Hz, H^5), 7.84 (1H, d, $^3J_{HH}$ = 6.0 Hz, $H^{6\prime\prime\prime}$), 7.80 (1H, d, $^3J_{HH}$ = 6.0 Hz, $H^{5\prime\prime}$), 7.60 (1H, d, $^3J_{HH}$ = 5.5 Hz, $H^{5\prime}$), 7.52 (1H, d, $^3J_{HH}$ = 6.0 Hz, $H^{6\prime\prime}$), 7.15 (1H, d, $^3J_{HH}$ = 6.0 Hz, $H^{5\prime\prime\prime}$), 6.59 (1H, tt, $^2J_{HF}$ = 50.8 Hz, $^3J_{HF}$ = 5.5 Hz, $H^{10\prime\prime\prime}$), 6.50 (1H, tt, $^2J_{HF}$ = 50.8 Hz, $^3J_{HF}$ = 5.5 Hz, $H^{10\prime\prime}$), 5.06 (2H, s, $H^{8\prime\prime\prime}$), 4.79 (2H, s, $H^{8\prime\prime}$), 4.37 (2H, t, $^3J_{HF}$ = 14.0 Hz, $H^{9\prime\prime\prime}$), 4.17 (2H, t, $^3J_{HF}$ = 14.0 Hz, $H^{9\prime\prime}$); δ_F (470.5 MHz, CD_3OD) −121.3 (2F, t, $^3J_{HF}$ = 12.7 Hz, $-CH_2\underline{C}F_2CF_2-$), −121.4 (2F, t, $^3J_{HF}$ = 13.5 Hz, $-CH_2\underline{C}F_2CF_2-$), −126.7 (2F, s, $-CH_2CF_2\underline{C}F_2-$), −126.9 (2F, s, $-CH_2CF_2\underline{C}F_2-$), −131.9 (2F, d, $-\underline{C}F_2CF_2H$), −132.0 (2F, d, $-\underline{C}F_2CF_2H$), −140.1 (1F, t, $^2J_{HF}$ = 45.2 Hz, $-\underline{C}F_2H$), 140.1 (1F, t, $^2J_{HF}$ = 40.1 Hz, $-\underline{C}F_2H$); δ_C (113 MHz, CD_3OD) 167 (C^7), 167 ($C^{7\prime}$), 160 (C^2), 160 ($C^{2\prime}$), 160 ($C^{2\prime\prime}$), 158 ($C^{2\prime\prime\prime}$), 155 (C^6), 154 ($C^{6\prime}$), 154 ($C^{6\prime\prime}$), 153 ($C^{6\prime\prime\prime}$), 150 (C^4), 149 ($C^{4\prime}$), 140 ($C^{4\prime\prime}$), 139 ($C^{4\prime\prime\prime}$), 127.0 (C^3), 126 ($C^{3\prime}$), 126 ($C^{3\prime\prime}$), 125 ($C^{3\prime\prime\prime}$), 124 (C^5), 124 ($C^{5\prime}$), 122 ($C^{5\prime\prime}$), 122 ($C^{5\prime\prime\prime}$), 135 (C^{14} of NCS), 134 ($C^{14\prime}$ of NCS), 106−118 ($C^{10\prime\prime\prime}$−$C^{13\prime\prime\prime}$ and $C^{10\prime\prime}$−$C^{13\prime\prime}$), 73 ($C^{8\prime\prime\prime}$), 73 ($C^{8\prime\prime}$), 69 ($C^{9\prime\prime\prime}$), 69 ($C^{9\prime\prime}$). FT-IR (cm^{-1}): 2105 [ν(N═C), s], 1718 [ν(bpy-C═O), s], 1613 [ν_{as}(bpy-COO^-), s], 1617, 1543, 1406 [ν(bpy), m], 1383 [ν(bpy-CH_2O), m], 1169 [$\nu(CF_2)$, vs], 1258, 1230 [ν(bpy-CO), s], 1126 [$\nu(CF_2)$, vs].

HR-MS (FAB), M^+: Calcd for $C_{36}H_{24}F_{16}N_6O_6RuS_2$: m/z 1105.9969. Found: m/z 1105.9962.

Analytical Data of CT4. δ_H (500 MHz, CD_3OD) 9.60 (1H, d, $^3J_{HH}$ = 5.5 Hz, H^6), 9.36 (1H, d, $^3J_{HH}$ = 5.5 Hz, $H^{6\prime}$), 9.00 (1H, s, H^3), 8.86 (1H, s, $H^{3\prime}$), 8.52 (1H, s, $H^{3\prime\prime\prime}$), 8.37 (1H, s, $H^{3\prime\prime}$), 8.22 (1H, d, $^3J_{HH}$ = 5.5 Hz, $H^{5\prime}$), 7.83 (1H, d, $^3J_{HH}$ = 5.5 Hz, $H^{6\prime\prime\prime}$), 7.81 (1H, d, $^3J_{HH}$ = 5.5 Hz, $H^{5\prime\prime}$), 7.61 (1H, d, $^3J_{HH}$ = 5.5 Hz, $H^{5\prime}$), 7.52 (1H, d, $^3J_{HH}$ = 5.5 Hz, $H^{6\prime\prime}$), 7.15 (1H, d, $^3J_{HH}$ = 5.5 Hz, $H^{5\prime\prime\prime}$), 6.59 (1H, tt, $^2J_{HF}$ = 52.5 Hz, $^3J_{HF}$ = 5.5 Hz, $H^{10\prime\prime\prime}$), 6.50 (1H, tt, $^2J_{HF}$ = 52.5 Hz, $^3J_{HF}$ = 5.5 Hz, $H^{10\prime\prime}$), 5.03 (2H, s, $H^{8\prime\prime\prime}$), 4.76 (2H, s, $H^{8\prime\prime}$), 4.19 (2H, t, $^3J_{HF}$ = 13.0 Hz, $H^{9\prime\prime\prime}$), 3.98 (2H, t, $^3J_{HF}$ = 13.0 Hz, $H^{9\prime\prime}$); δ_F (470.5 MHz, CD_3OD) −127.3 (2F, m, $-CH_2CF_2CF_2H$), −127.5 (2F, m, $-CH_2CF_2CF_2H$), −141.8 (2F, t, $^2J_{HF}$ = 51.8 Hz, $-\underline{C}F_2H$), −141.8 (2F, t, $^2J_{HF}$ = 51.8 Hz, $-\underline{C}F_2H$); δ_C (113 MHz, CD_3OD) 167 (C^7), 167 ($C^{7\prime}$), 161 (C^2), 160 ($C^{2\prime}$), 160 ($C^{2\prime\prime}$), 158 ($C^{2\prime\prime\prime}$), 155 (C^6), 154 ($C^{6\prime}$), 154 ($C^{6\prime\prime}$), 153 ($C^{6\prime\prime\prime}$), 150 (C^4), 149 ($C^{4\prime}$), 140 ($C^{4\prime\prime}$), 140 ($C^{4\prime\prime\prime}$), 127 (C^3), 126 ($C^{3\prime}$), 126 ($C^{3\prime\prime}$), 125 ($C^{3\prime\prime\prime}$), 124 (C^5), 124 ($C^{5\prime}$), 122 ($C^{5\prime\prime}$), 122 ($C^{5\prime\prime\prime}$), 135 ($C^{12\prime}$ of NCS), 134 (C^{12} of NCS), 106−118 ($C^{10\prime\prime\prime}$, $C^{11\prime\prime\prime}$ and $C^{10\prime\prime}$, $C^{11\prime\prime}$), 73 ($C^{8\prime\prime\prime}$), 73 ($C^{8\prime\prime}$), 69 ($C^{9\prime\prime\prime}$), 69 ($C^{9\prime\prime}$). FT-IR (cm^{-1}): 2105 [ν(N═C), s], 1718 [ν(bpy-C═O), s], 1617, 1548, 1407 [ν(bpy), m], 1613 [ν_{as}(bpy-COO^-), s], 1624, 1561 [ν(bpy), m], 1384 [ν(bpy-CH_2O), m], 1244, 1200, 1145 [$\nu(CF_2)$, vs], 1373 [ν_s(bpy-COO^-), s], 1260, 1230 [ν(bpy-CO), s], 1104 [$\nu(CF_2)$, vs]. HR-MS (FAB), M^+: Calcd for $C_{32}H_{24}F_8N_6O_6RuS_2$: m/z 906.0114. Found: m/z 906.0115.

Electrochemistry. Electrochemical data were obtained by CV using a CH Instruments model 660A potentiostat. Glassy carbon was used as the working electrode, Ag/AgCl was the reference electrode, and platinum wire was used as the counter electrode. The sensitizers (0.001 M) were dissolved in DMF containing 0.1 M tetrabutylammonium tetrafluoroborate ($TBABF_4$) as the electrolyte. After measurement, ferrocene was added as the internal reference for calibration. The scan rate was between 0.1 and 0.5 V s^{-1}.

Fabrication and Characterization of DSCs. The TiO_2 paste, which was prepared according to the method developed by Lin et al., was then deposited on a FTO glass substrate by the glass rod method with a dimension of 0.25 cm^2. The TiO_2-coated FTO was heated to 500 °C at a heating rate of 10 °C min^{-1} and maintained for 30 min before being cooled to room temperature. The thickness of the TiO_2 film was controlled by repeating the procedure described above. A thermally platinized FTO was used as a counter electrode and was controlled to have an active area of 0.36 cm^2 by adhered polyester tape with a thickness of 60 μm. After heating of the TiO_2 thin film to 80 °C, the film was removed from the oven and dipped into a THF solution containing 3 × 10^{-4} M dye sensitizers for at least 12 h. Because of the higher solubility of the sensitizers in THF, THF was used as a dipping solution to ensure enough uptake of the sensitizers. After a THF rinse, the photoanode was placed on top of the counter electrode and tightly clipped to it to form a cell. The electrolyte was then injected into the space and the cell sealed with Torr Seal cement (Varian, MA). The electrolyte was composed of 0.5 M lithium iodide (LiI), 0.05 M iodine (I_2), and 0.5 M 4-*tert*-butylpyridine dissolved in acetonitrile. A 0.6 × 0.6 cm^2 cardboard mask was clipped onto the device to constrain the illumination area. The photoelectrochemical characterizations on the solar cells were carried out by using an Oriel class A solar simulator (Oriel 91195A, Newport Corp.). Photocurrent−voltage characteristics of the DSCs were recorded with a potentiostat/galvanostat (CHI 650B, CH Instruments) at a light intensity of 1.0 sun calibrated by an Oriel reference solar cell (Oriel 91150, Newport Corp.). The monochromatic quantum efficiency was recorded through a monochromator (Oriel 74100, Newport Corp.) at short-circuit conditions. The intensity of each wavelength was in the range of 1−3 mW cm^{-2}.

Measurement of the Adsorbed Density of Each Dye. The adsorbed density of each dye was calculated from the difference in the concentration of each solution before (3 × 10^{-4} M) and after TiO_2 film immersion. The thickness and area of the TiO_2 film were controlled at ca. 14 μm and ca. 2 cm^2, respectively. After TiO_2 film immersion for 16 h, the FTO glass was removed from the dye solution and was dried in air (or inside an oven); then the dye-adsorbed TiO_2 was totally scratched out from the FTO glass, and the weight of the scratched TiO_2 with adsorbed dye was taken. Then the number of moles of dye anchoring on TiO_2 per square centimeter was calculated by the following equation: [moles of absorbed dye on TiO_2/wt of (TiO_2 + adsorbed dye)] × 2.4. (Note: on average, every square centimeter of TiO_2 on the device weighs 2.4 mg.)

IR Spectrum of the Adsorbed Dye. After the TiO_2-adsorbed dye (or dye salt) was totally scratched out from the FTO glass and the weight of the scratched dye (or dye salt) was taken, the scratched dye (or dye salt) was then used for the FT-IR measurement using the ATR mode. Then the IR spectrum of the adsorbed dye was compared with that of free dye.

■ ASSOCIATED CONTENT

Supporting Information. Some experimental data, the combined absorption and emission spectra of CT dyes, and some ATR-FT-IR spectra of the TBA salts of free and adsorbed dyes. This material is available free of charge via the Internet at http://pubs.acs.org.

■ AUTHOR INFORMATION

Corresponding Author

*E-mail: normanlu@ntut.edu.tw (N.L.), jtlin@sinica.edu.tw (J.T.L.). Fax: (+886)2-2731-7174. Phone: (+886)2-2771-2171 ext. 2417.

■ ACKNOWLEDGMENT

The authors thank the NSC for financial support. Also, we thank Raymond L. Sobocinski (E.I. du Pont de Nemours) for proofreading the manuscript.

■ REFERENCES

(1) O'Regan, B.; Grätzel, M. *Nature* **1991**, *353*, 737.
(2) Grätzel, M. *Nature* **2001**, *414*, 338.
(3) Zhang, G.; Bala, H.; Cheng, Y.; Shi, D.; Lv, X.; Yu, Q.; Wang, P. *Chem. Commun.* **2009**, 2198.
(4) Choi, H.; Raabe, I.; Kim, D.; Teocoli, F.; Kim, C.; Song, K.; Yum, J.-H.; Ko, J.; Nazeeruddin, M. K.; Grätzel, M. *Chem.—Eur. J.* **2010**, *16*, 1193.
(5) Cao, Y.; Bai, Y.; Yu, Q.; Cheng, Y.; Liu, S.; Shi, D.; Gao, F.; Wang, P. *J. Phys. Chem. C* **2009**, *113*, 6290.
(6) Chiba, Y.; Islam, A.; Watanabe, Y.; Komiya, R.; Koide, N.; Han, L. *Jpn. J. Appl. Phys., Part 2* **2006**, *45*, L638.
(7) Nazeeruddin, M. K.; Kay, A.; Rodicio, I.; Humphry-Baker, R.; Müller, E.; Liska, P.; Vlachopoulos, N.; Grätzel, M. *J. Am. Chem. Soc.* **1993**, *115*, 6382.
(8) Nazeeruddin, M. K.; Péchy, P.; Renouard, T.; Zakeeruddin, S. M.; Humphry-Baker, R.; Comte, P.; Liska, P.; Cevey, L.; Costa, E.; Shklover, V.; Spiccia, L.; Beacon, G. B.; Bignozzi, A.; Grätzel, M. *J. Am. Chem. Soc.* **2001**, *123*, 1613.
(9) Wang, P.; Zakeeruddin, S. M.; Moser, J. E.; Humphry-Baker, R.; Comte, P.; Aranyos, V.; Hagfeldt, A.; Nazeeruddin, M. K.; Grätzel, M. *Adv. Mater.* **2004**, *16*, 1806.
(10) Nazeeruddin, M. K.; De Angelis, F.; Fantacci, S.; Selloni, A.; Viscardi, G.; Liska, P.; Ito, S.; Takeru, B.; Grätzel, M. *J. Am. Chem. Soc.* **2005**, *127*, 16835.
(11) Wang, P.; Zakeeruddin, S. M.; Moser, J. E.; Nazeeruddin, M. K.; Sekiguchi, T.; Grätzel, M. *Nat. Mater.* **2003**, *2*, 402.
(12) Wang, P.; Klein, C.; Humphry-Baker, R.; Zakeeruddin, S. M.; Grätzel, M. *J. Am. Chem. Soc.* **2005**, *127*, 808.
(13) To the best of our knowledge, there are only two literature accounts showing the similar Ru complex with the monosubstituted fluorous chain but not with the bis-substituted chains. These two accounts are as follows: (a) Lagref, J.-J.; Nazeeruddin, M. K.; Grätzel, M. *Inorg. Chim. Acta* **2008**, *361*, 735. (b) Lagref, J.-J.; Nazeeruddin, M. K.; Grätzel, M. *Synth. Met.* **2003**, *138*, 333.
(14) Lu, N.; Lin, Y.-C.; Chen, J.-Y.; Chen, T.-C.; Chen, S.-C.; Wen, Y.-S.; Liu, L.-K. *Polyhedron* **2007**, *26*, 3045.
(15) Kuang, D.; Ito, S.; Wenger, B.; Klein, C.; Moser, J.; Humphry-Baker, R.; Zakeeruddin, S. M.; Grätzel, M. *J. Am. Chem. Soc.* **2006**, *128*, 4146.
(16) (a) Nazeeruddin, M. K.; Zakeeruddin, S. M.; Lagref, J.-J.; Liska, P.; Comte, P.; Barolo, C.; Viscardi, G.; Schenk, K.; Grätzel, M. *Coord. Chem. Rev.* **2004**, *248*, 1317.(b) Ito, S.; Nazeeruddin, M. K.; Zakeeruddin, S.; Péchy, P.; Comte, P.; Grätzel, M.; Mizuno, T.; Tanaka, A.; Koyanagi, T. *Int. J. Photoenergy* **2009**, art. no. 517609. (c) Yu, Q.; Liu, S.; Zhang, M.; Cai, N.; Wang, Y.; Wang, P. *J. Phys. Chem. C* **2009**, *113*, 14559.
(17) Jang, S.-R.; Yum, J.-H.; Klein, C.; Kim, K.-J.; Wagner, P.; Officer, D.; Grätzel, M.; Nazeeruddin, M. K. *J. Phys. Chem. C* **2009**, *113*, 1998.
(18) Bard, A. J.; Faulkner, L. R. *Electrochemical Methods: Fundamentals and Applications*, 2nd ed.; Wiley: Weinheim, Germany, 2001.
(19) Nazeeruddin, M. K.; De Angelis, F.; Fantacci, S.; Selloni, A.; Viscardi, G.; Liska, P.; Ito, S.; Takeru, B.; Grätzel, M. *J. Am. Chem. Soc.* **2005**, *127*, 16835.
(20) Kong, F.; Dai, S.; Wang, K. *Adv. Optoelectron.* **2007**, art. no. 75384.
(21) (a) Lu, N.; Tu, W.-H.; Wen, Y.-S.; Liu, L.-K.; Chou, C.-Y.; Jiang, J.-C. *CrystEngComm* **2010**, *12*, 538. (b) Lu, N.; Hou, H.-C.; Lin, C.-T.; Li, C.-K.; Liu, L.-K. *Polyhedron* **2010**, *29*, 1123.
(22) Thomas, K. R. J.; Hsu, Y.-C.; Lin, J. T.; Lee, K.-M.; Ho, K.-C.; Lai, C.-H.; Cheng, Y.-M.; Chou, P.-T. *Chem. Mater.* **2008**, *20*, 1830.
(23) Hirose, F.; Kuribayashi, K.; Suzuki, T.; Narita, Y.; Kimura, Y.; Michio Niwano, M. *Electrochem. Solid-State Lett.* **2008**, *11*, A109.
(24) Hirose, F.; Kuribayashi, K.; Shikaku, M.; Narita, Y.; Takahashi, Y.; Kimura, Y.; Niwano, M. *J. Electrochem. Soc.* **2009**, *156*, B987.
(25) It was reported that the length of the alkyl chain did not affect charge recombination: Mori, S. N.; Kubo, W.; Kanzaki, T.; Masaki, N.; Wada, Y.; Yanagida, S. *J. Phys. Chem. C* **2007**, *111*, 3522.

■ NOTE ADDED AFTER ASAP PUBLICATION

This paper was published on the Web on April 14, 2011, with a minor error in Figure 1. The corrected version was reposted on May 9, 2011.